ORIGINAL RESEARCH

Repeated Mouse Lung Exposures to *Stachybotrys chartarum* Shift Immune Response from Type 1 to Type 2

Jamie H. Rosenblum Lichtenstein[1]*, Ramon M. Molina[1], Thomas C. Donaghey[1], Yi-Hsiang H. Hsu[1,2], Joel A. Mathews[1], David I. Kasahara[1], Jin-Ah Park[1], André Bordini[1], John J. Godleski[1], Bruce S. Gillis[3], and Joseph D. Brain[1]

[1]Molecular and Integrative Physiological Sciences Program, Department of Environmental Health, Harvard T.H. Chan School of Public Health, Boston, Massachusetts; [2]Hebrew SeniorLife Institute for Aging Research and Harvard Medical School, Boston, Massachusetts; and [3]Department of Medicine, University of Illinois College of Medicine, Chicago, Illinois

Abstract

After a single or multiple intratracheal instillations of *Stachybotrys chartarum* (*S. chartarum* or black mold) spores in BALB/c mice, we characterized cytokine production, metabolites, and inflammatory patterns by analyzing mouse bronchoalveolar lavage (BAL), lung tissue, and plasma. We found marked differences in BAL cell counts, especially large increases in lymphocytes and eosinophils in multiple-dosed mice. Formation of eosinophil-rich granulomas and airway goblet cell metaplasia were prevalent in the lungs of multiple-dosed mice but not in single- or saline-dosed groups. We detected changes in the cytokine expression profiles in both the BAL and plasma. Multiple pulmonary exposures to *S. chartarum* induced significant metabolic changes in the lungs but not in the plasma. These changes suggest a shift from type 1 inflammation after an acute exposure to type 2 inflammation after multiple exposures to *S. chartarum*. Eotaxin, vascular endothelial growth factor (VEGF), MIP-1α, MIP-1β, TNF-α, and the IL-8 analogs macrophage inflammatory protein-2 (MIP-2) and keratinocyte chemoattractant (KC), had more dramatic changes in multiple-than in single-dosed mice, and parallel the cytokines that characterize humans with histories of mold exposures versus unexposed control subjects. This repeated exposure model allows us to more realistically characterize responses to mold, such as cytokine, metabolic, and cellular changes.

Keywords: metabolome; lymphoid cells; fungi; macrophages; inflammation

Stachybotrys chartarum is a mold that is most problematic in indoor environments (1). It is associated with pulmonary responses, such as asthma, pulmonary hemorrhage, inflammation, runny nose, and cough, in both humans and mice (2, 3). Children exposed to *S. chartarum* at school are at increased risk of asthma (4, 5), and *S. chartarum* was reported to increase risk of infant idiopathic pulmonary hemorrhage, although coexposures may also be important (6). *S. chartarum* produces proteins, including SchS21, a DNase, and SchS34 (unknown function), that have been shown to be antigenic in both humans and animals (7). Macrocyclic trichothecene mycotoxins produced by *S. chartarum*, such as satratoxin G, have been shown to induce apoptosis (8). Exposures are almost always chronic and low level; unfortunately, evaluations of airborne mold are usually lacking (9). *S. chartarum* grows amid other pathogens, making it difficult to identify health effects solely attributable to *S. chartarum*.

Experimental exposures of mice to *S. chartarum* or extracts have typically

Clinical Relevance

This study showed distinct inflammatory and metabolomic profiles that were consistent with a shift from a type 1 immune response after a single exposure to *Stachybotrys chartarum* to a type 2 immune response after multiple exposures. Future studies should focus on the impact of multiple rather than single acute exposures, and caution should be exercised when interpreting responses to acute exposures in animal and human studies.

involved only a single acute exposure (10–15). Few studies include multiple exposures to intact *S. chartarum*; we found four (16–19). None compared single with multiple exposures, and only two (16, 17) included measurements of cytokines, such as IL-4, IL-5, and INF-γ.

We sought to characterize cytokines, metabolites, and inflammatory patterns reflected in bronchoalveolar lavage (BAL), lung tissue, and plasma after single versus multiple doses of intratracheally instilled *S. chartarum* spores. We compared responses to single and multiple doses of *S. chartarum* to the cytokine and chemokine profiles that have been previously reported in humans with a history of mold exposures (9).

Materials and Methods

We studied three groups of mice intratracheally instilled with *S. chartarum* weekly for 7 weeks (multiple-dosed), with saline weekly for 6 weeks followed by a single intratracheal instillation of *S. chartarum* in the 7th week (single-dosed), and with saline weekly for 7 weeks (vehicle control). At the end of each treatment, we measured the responses of 32 cytokines in BAL and plasma. We also employed global metabolomic profiling to examine changes in lungs and plasma and flow cytometry to identify the lymphocytes recovered from lung parenchyma. Our goal is to integrate the cytokine and metabolic results with the cellular responses.

Spore Intratracheal Instillations

Male BALB/c mice (7 wk old; Taconic Farms, Germantown, NY) were housed at

Table 1. Pathway Analysis of Metabolites in the Lungs

Pathway Name	Total No. of Metabolites in Pathway	Hits	P Value	FDR q Value	KEGG Pathway
Glutathione metabolism	26	7	1.78E−06	5.22E−05	mmu00480
Arachidonic acid metabolism	36	5	2.19E−06	5.22E−05	mmu00590
Starch and sucrose metabolism	19	4	3.64E−06	5.22E−05	mmu00500
Amino sugar and nucleotide sugar metabolism	37	6	3.70E−06	5.22E−05	mmu00520
Arginine and proline metabolism	44	13	4.21E−06	5.22E−05	mmu00330
Pentose and glucuronate interconversions	16	3	7.73E−06	7.99E−05	mmu00040
Pyrimidine metabolism	41	11	2.73E−05	2.42E−04	mmu00240
Ascorbate and aldarate metabolism	9	5	4.66E−05	3.21E−04	mmu00053
Glycine, serine, and threonine metabolism	31	8	5.78E−05	3.59E−04	mmu00260
Fructose and mannose metabolism	21	3	1.48E−04	8.23E−04	mmu00051
Galactose metabolism	26	5	1.59E−04	8.23E−04	mmu00052
Glycerolipid metabolism	18	3	1.78E−04	8.50E−04	mmu00561
Pyruvate metabolism	23	4	2.33E−04	0.00103	mmu00620
Biosynthesis of unsaturated fatty acids	42	11	2.86E−04	0.00118	mmu01040
Pantothenate and CoA biosynthesis	15	9	4.26E−04	0.00165	mmu00770
Inositol phosphate metabolism	28	4	4.53E−04	0.00165	mmu00562
Glyoxylate and dicarboxylate metabolism	18	5	6.10E−04	0.00210	mmu00630
Glycolysis or gluconeogenesis	26	3	0.00119	0.00388	mmu00010
Fatty acid biosynthesis	43	6	0.00267	0.00827	mmu00061
Fatty acid metabolism	39	4	0.00304	0.00898	mmu00071
Butanoate metabolism	22	3	0.00340	0.00958	mmu00650
Fatty acid elongation in mitochondria	27	2	0.00430	0.0114	mmu00062
Methane metabolism	9	2	0.00458	0.0114	mmu00680
Cyanoamino acid metabolism	6	2	0.00458	0.0114	mmu00460
Citrate cycle (TCA cycle)	20	4	0.00491	0.0117	mmu00020
Lysine degradation	23	5	0.00580	0.0133	mmu00310
Tryptophan metabolism	40	4	0.00644	0.0137	mmu00380
Valine, leucine and isoleucine degradation	38	4	0.00665	0.0137	mmu00280
α-Linolenic acid metabolism	9	2	0.00746	0.0149	mmu00592
Propanoate metabolism	20	3	0.00911	0.0176	mmu00640
Cysteine and methionine metabolism	27	5	0.00951	0.0178	mmu00270
Steroid biosynthesis	35	3	0.0105	0.0193	mmu00100
Synthesis and degradation of ketone bodies	5	2	0.0118	0.0209	mmu00072
Primary bile acid biosynthesis	46	5	0.0126	0.0217	mmu00120

Definition of abbreviations: CoA, coenzyme A; FDR, false discovery rate; KEGG, Kyoto Encyclopedia of Genes and Genomes; TCA, tricarboxylic acid.
Pathway analysis was performed based on KEGG metabolic pathways. Total number of metabolites in pathway indicates the number of known metabolites in the KEGG database. "Hits" indicates the number of the observed (measured) metabolites in our study listed in the KEGG pathways.

our animal facility and were acclimatized for 1 week before the experiment. The Harvard Medical Area Standing Committee on Animal Use and Care (Boston, MA) approved the protocol. All mice, while anesthetized, received intratracheal instillations of the designated exposure (2.5 ml/kg body weight saline or 2.5×10^5 spores/ml) once per week in the morning for 7 weeks (20). Tissue harvests for all analyses were performed 24 hours after the last instillation.

BAL, Lung and Plasma Collection, Analyses, and Histopathology

Mice from each of the three exposure groups were randomized to BAL ($n = 11$/exposure group) or whole-lung metabolomics analysis ($n = 10$/exposure group). All mice were killed with isoflurane anesthesia followed by collection of blood through the abdominal aorta. Lungs were lavaged (13) and a subset of lavaged lungs ($n = 6$/exposure group) was dissected for lymphocyte isolation and subtyping. Matched plasma samples were also collected. Lungs from single- and multiple-dosed groups were fixed in 10% formalin and embedded in paraffin, sectioned, and then stained with hematoxylin and eosin, Giemsa, periodic acid Schiff (PAS) and Grocott's methenamine silver (GMS) for specific fungal staining. BAL and plasma samples were sent to Eve Technologies (Calgary, AB, Canada) for cytokine analyses using a mouse 32-plex array. Whole lungs and plasma were sent to Metabolon, Inc. (Research Triangle Park, NC) for global metabolomic analyses (21–23).

Flow Cytometry

Cell suspensions from disaggregated lungs were stimulated with ionomycin and phorbol 12-myristate 13-acetate in the presence of GolgiStop (24, 25). Cells were fixed, permeabilized, and stained for surface markers (CD45, CD3, CD4, CD69, and TCRd) and intracellular cytokines (IL-13 and IL-17), then analyzed (BD Canto II cytometer, BD DIVA, and FlowJo; BD Biosciences, San Jose, CA). Stained cells were gated by size and complexity (side scatter–forward scatter), followed by gating for CD45^{+} and CD3^{+} cells. Among CD3^{+} cells, we identified IL-17A^{+} and IL-13^{+} cells.

Statistical Analyses

Single-marker analyses by ANOVA, principal component analysis (PCA), hierarchical clustering (heat map), and support vector machine (SVM) analysis were employed to identify cell, cytokine, and metabolite signatures associated with each treatment. Pathway analysis using Kyoto Encyclopedia of Genes and Genomes (KEGG) maps was employed to identify pathways altered by repeated exposures to *S. chartarum* (Table 1). Details are provided in the online supplement.

Results

BAL Analyses

Higher neutrophil counts were observed in both single- and multiple-dosed mice compared with saline controls, although not different between the two spore-dosed groups (Figure 1A). There was a slight increase in BAL lymphocytes and eosinophils in the single-dosed mice, although this response was small compared with that seen after the same challenge in the multiple-dosed animals. Lymphocytes increased 33-fold and eosinophils increased 39-fold in the multiple- versus the single-dosed animals (Figure 1A). Macrophage numbers did not differ among the different exposure groups. Lactate dehydrogenase (cytotoxicity) levels were higher in multiple-dosed mice (false discovery rate [FDR] q value < 0.05) (Figure 1B). Myeloperoxidase (neutrophil degranulation) was similar in single- and multiple-dosed mice, but was higher than in vehicle controls (Figure 1B).

A total of 18 out of 32 measured cytokines and chemokines in the BAL were significantly increased in both groups instilled with spores (ANOVA, FDR adjusted $q < 0.05$) versus saline control. Some cytokines and chemokines (eotaxin, IL-4, IL-6, IL-5, monocyte chemoattractant protein-1 [MCP-1], IL-13, IL-10, IL-9, and M-CSF) were highest in multiple-dosed mice (Figures 2A and 2B). Others (TNF-α, lipopolysachharide-induced CXC [LIX],
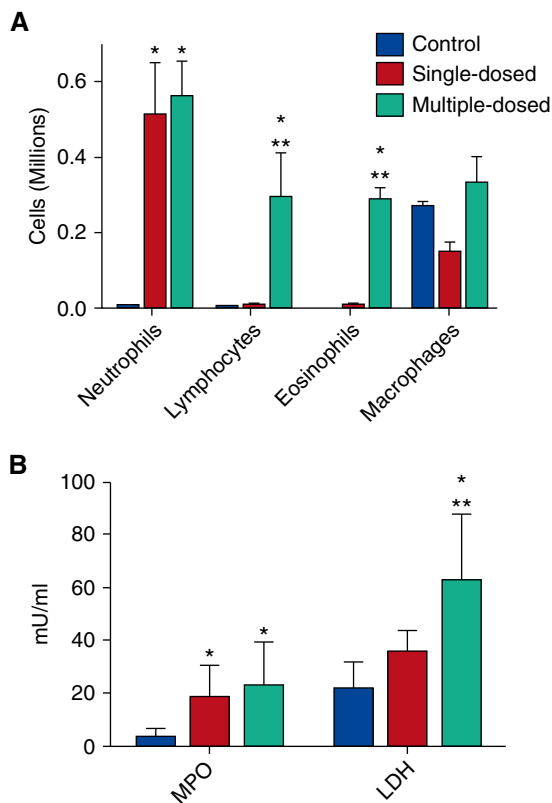

Figure 1. Bronchoalveolar lavage (BAL) analysis at 24 hours after the final intratracheal instillation. (*A*) Differential cell counts. (*B*) Myeloperoxidase (MPO) and lactate dehydrogenase (LDH) (mU/ml). *Adjusted false discovery rate (FDR) q value < 0.05 versus control; **adjusted FDR q value < 0.05 versus single-dosed mice; two-way ANOVA. Data are mean (±SE); $n = 10–12$.
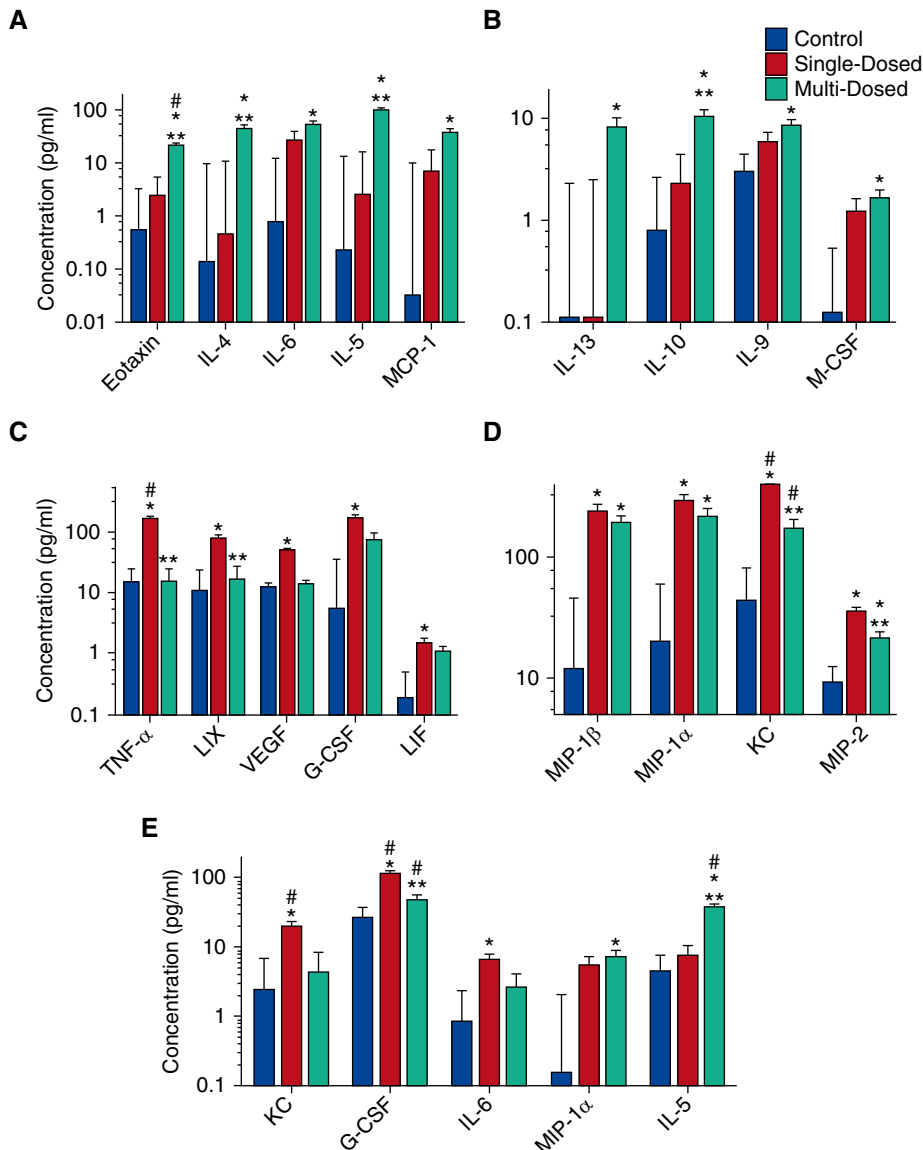
Figure 2. (A–E) BAL cytokine analysis at 24 hours after the final intratracheal instillation. (A and B) Cytokines that were increased in multiple- compared with single-dosed mice. A and B have different scales. (C) Cytokines that were increased in single- compared with multiple-dosed mice. (D) Increased cytokines in both spore-exposed groups compared with controls. (E) Plasma cytokines 24 hours after final intratracheal instillation. All values are mean (±SE). *ANOVA FDR q value < 0.05 versus control; **ANOVA FDR q value < 0.05 versus single-dosed; #multiple marker analysis area under the curve top hits. G-CSF, granulocyte colony-stimulating factor; KC, keratinocyte chemoattractant; LIF, leukemia inhibitory factor; LIX, lipopolysachharide-induced CXC; MCP, monocyte chemoattractant protein; M-CSF, macrophage colony-stimulating factor; MIP, macrophage inflammatory proteins; VEGF, vascular endothelial growth factor.

control mice with 80% accuracy. When KC and eotaxin were combined, single-dosed mice could be distinguished from controls with 98% accuracy. TNF-α, eotaxin, and KC provided the highest accuracy to distinguish mice among the three exposure groups.

Blood Cell Counts and Cytokine Levels in Plasma
No significant differences in peripheral blood cell counts were observed among the three groups (data not shown). Five cytokines measured in plasma (KC, G-CSF, IL-6, MIP-1α, and IL-5) were significantly higher in both single- and multiple-dosed animals compared with saline controls (Figure 2E). IL-5 was higher and KC was lower in the plasma of multiple- compared with single-dosed mice (Figure 2E). Based on SVM analyses, IL-5 and KC together differentiate multiple- from single-dosed mice with 71% accuracy. IL-5 alone differentiated multiple-dosed from control mice with 80% accuracy.

Flow Cytometric Analyses
Eosinophil and neutrophil influx into the lungs, seen in the multiple-dosed group (Figure 1A), is usually controlled by the Th2 (IL-13) and Th17 (IL-17) pathways (25–28). To determine if the numbers of IL-13^{+} and IL-17A^{+} cells in lung tissue were altered, we analyzed disaggregated cells using flow cytometry. We found that in the multiple-dosed group there was no increase in CD45^{+} or CD45^{+}CD3^{+} cells (Figures 3A and 3B). In contrast, there were increased numbers of CD45^{+}CD3^{+}IL-13^{+} cells in the multiple-dosed mice versus the control or the single-dose groups (Figure 3C). The numbers of CD45^{+}CD3^{+}IL-17A^{+} (Th17) cells did not change (Figure 3D). However, in the multiple-dosed group, we saw a dramatic increase in the number of CD45^{+}CD3^{−}IL-17A^{+} cells compared with the single-dosed and saline groups (Figure 3E). In addition, we also gated on total and activated γδ T cells and found that the total numbers of γδ T cells, as well as activated γδ T cells, were increased in the multiple-dosed mice compared with either the single-dosed or vehicle-only mice (see Figure E2 in the online supplement). Although we did not stain the γδ T cells for IL-13 or IL-17A, activated γδ T cells can produce both (29, 30), and are also a possible source of both IL-13 and IL-17A.

vascular endothelial growth factor [VEGF], granulocyte-colony stimulating factor [G-CSF], and leukemia inhibitory factor [LIF]) were lower in multiple-dosed mice (Figure 2C), whereas still others (macrophage inflammatory proteins [MIP]-1α, MIP-1β, keratinocyte chemoattractant [KC], and MIP-2) were

significantly higher in both spore-dosed groups than in the control group (Figure 2D). In multiple-marker analyses, we found that TNF-α and eotaxin together differentiate multiple- from single-dosed mice with 100% accuracy based on cross-validation analyses in SVM models. Eotaxin alone distinguished multiple-dosed from
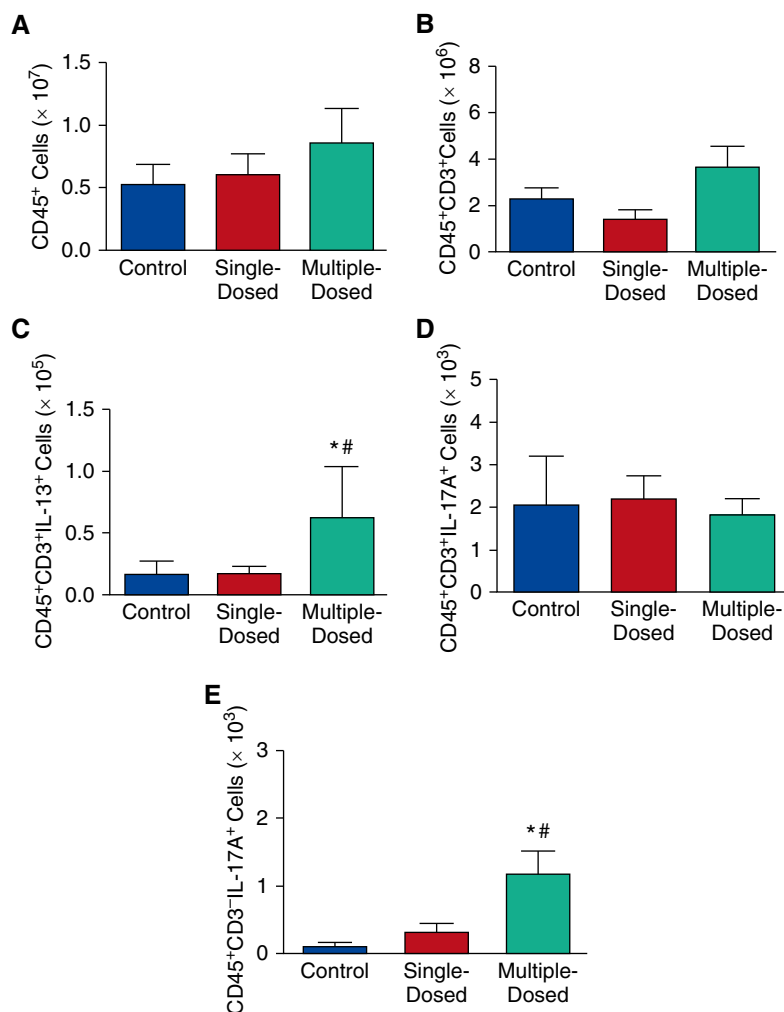
Figure 3. Flow cytometric analysis of lung cells. (*A*) Total leukocyte counts, (*B*) total T lymphocyte counts, (*C*) total numbers of T helper type 2 (Th2) cells, (*D*) total numbers of Th17 cells, and (*E*) numbers of probable innate lymphoid cell 3 cells. Data are mean (±SE); $n = 5$–6. *$P < 0.05$ versus control mice; #$P < 0.05$ versus single-dosed mice.

Histopathology

Histopathologic examinations of lung sections showed significantly more granulomas with eosinophils in multiple-dosed (Figure 4B) than in single-dosed mice (Figure 4A). There were roughly five times more granulomas in multiple-dosed than in single-dosed lungs. Multiple spores and fragments present within the granulomas were visible in GMS-stained sections (Figure 4C), hematoxylin and eosin–stained (Figures 4D and 4E), and Giemsa-stained sections (Figures 4F and 4G). Macrophages, multinucleate giant cells, eosinophils, and lymphocytes were present in the granulomas. Periodic acid Schiff, a goblet cell stain, demonstrated goblet cell metaplasia in the lungs of multiple-dosed (Figures 5B and 5D), but not single-dosed,

mice (Figures 5A and 5C). Goblet cell metaplasia is an example of remodeling seen in chronic airway diseases.

Metabolomic Analyses of Whole Lung and Plasma

We identified 325 measurable metabolites in the lungs and 344 in plasma. An unadjusted Welch's two-sample *t* test (Table E3) showed that 148 metabolites in the lungs were significantly different between multiple-dosed mice and control mice, and 146 metabolites were significantly different between multiple-dosed and single-dosed mice. We found 34 lung metabolites that were significantly different between single-dosed mice and control mice. In the plasma, we found significant differences in 31 metabolites between single-dosed and

control mice, 30 metabolites between multiple-dosed and single-dosed mice, and 10 metabolites between multiple-dosed and control mice.

PCA showed that multiple-dosed mice had significantly different metabolites in the lungs compared with both single-dosed and saline control mice, suggesting that lungs of the multiple-dosed mice have distinct biochemical pathways (Figure 6A). However, similar metabolomic differences in the plasma were not found among the three exposure groups (Figure 6B). Principal component 1 (Figure 6A) was able to differentiate mice with multiple exposures from the other groups through metabolite differences in docosahexaenoate (22:6n3), γ-glutamylglutamine, cytidine-3′-monophosphate, guanosine-3′-monophosphate, adenosine-3′-monophosphate, prostaglandin E1, prostaglandin A2, putrescine, prostaglandin E2, N-acetylneuraminate, and prostaglandin B2. These metabolites had an absolute eigenvalue greater than 0.1 in the PCA analysis.

We performed a cluster analysis using the 113 lung metabolites with an FDR *q* value less than 0.05 to identify patterns that differentiate the three groups of mice (Figure 6C). The multiple-dosed mice had two clusters of up-regulated metabolites and one of down-regulated metabolites compared with the single-dosed or saline control mice. Cluster analyses based on metabolites with FDR *q* value less than 0.05 confirmed the difference in pulmonary metabolites between multiple-versus single-dosed and saline control mice. Similar cluster analysis using the top 50 (Figure 6D) and top 10 plasma metabolites with an FDR *q* value less than 0.05 (data not shown) showed no clear differences between the two groups.

The Kyoto Encyclopedia of Genes and Genomes pathway analysis identified 34 pathways that significantly distinguished the multiple- from single-dosed mice based on metabolites measured in the lungs with an FDR *q* value less than 0.05 (Table 1). In the plasma, the only metabolic pathway with an FDR *q* value less than 0.05 was protein biosynthesis (FDR *q* value = 4.6×10^{-6}). Protein biosynthesis in the lungs was not altered significantly. No individual metabolite in the plasma was significantly different in any of the groups of mice (FDR *q* value < 0.05).
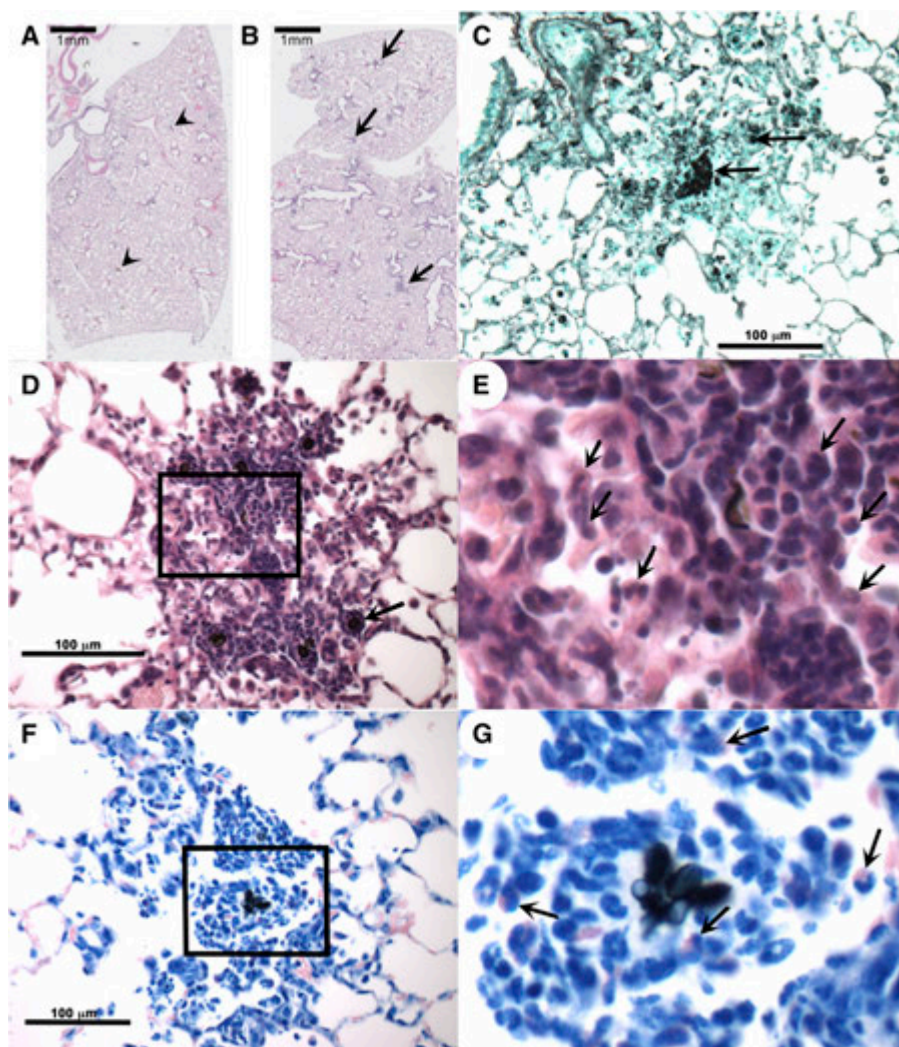
Figure 4. Histopathology of mouse lungs at 24 hours after final intratracheal instillation. (*A* and *B*) Overview of hematoxylin and eosin (H&E)–stained lung from single-dosed (*A*) and multiple-dosed (*B*) mice, showing foci of granulomas (*arrows*). *Scale bar* = 1 mm. *Arrowheads* indicate smaller granulomas. There were approximately 5 granulomas in single-dosed lungs and 25 granulomas in multiple-dosed lungs (*arrows*). (*C*) Grocott's methenamine silver–stained section shows mold spores in granulomas and macrophages in multiple-dosed mouse (*arrows*). *Scale bar* = 100 μm. (*D* and *F*) Multiple-dosed mouse lung shows an eosinophil-rich granuloma and numerous eosinophils (*arrows*) in H&E- (*D*) and Giemsa-stained (*F*) sections. *Scale bar* = 100 μm. (*E* and *G*) Higher magnification of the *enclosed areas* in *D* and *F* clearly shows eosinophils (*arrows*).

In lung tissue, our metabolomics data suggested that several pathways were altered. We found significant increases in prostaglandins D2, E1, and E2 (1.2- to 1.3-fold versus saline control) after a single exposure to *S. chartarum*, whereas, in the multiple-dosed group, prostaglandins A2, B2, D2, E1, E2, I2, F1α, and 15-hydroxyeicosatetraenoic acid (15-HETE) increased 1.4- to 3.6-fold compared with the single-dosed animals (Table E4). Nucleic acid synthesis pathways also differed. Between

multiple- and single-dosed mouse lungs, the three metabolites with both the largest fold change (five- to eightfold increase in multiple-dosed mice) and the lowest *P* values ($P < 10^{-9}$) were guanosine-3′-monophosphate, adenosine-3′-monophosphate, and cytidine-3′-monophosphate, all of which are involved in nucleotide metabolism (Figure E3C). Finally, we saw significant reductions in free fatty acids in the multiple-dosed compared with the single-dosed or control mice (Table 2 and Table E6).

When plasma data were analyzed, the metabolite with the lowest *P* value was ectoine, a xenobiotic that is most often associated with bacteria (31) (Table 2 and Figure E3F). Volcano plots identified many of the same metabolites, as did PCA and SVM analyses, as most significant in separating multiple- from single-dosed and control mice in both lungs and plasma (Figure E3).

Discussion

Naive mice exposed to *S. chartarum* for the first time responded very differently than mice that had been exposed repeatedly before their final challenge. We observed evidence for a change in the type of inflammation from a type 1 response in acutely exposed mice to a type 2 response in repeatedly exposed mice. The repeatedly exposed mice had decreased levels of TNF-α, which is associated with a type 1 immune response, and increased levels of eosinophils and IL-4, IL-5, and IL-13, which are associated with a type 2 immune response (32), compared with the single-dosed mice. The inflammation was probably mediated in part by *S. chartarum* mycotoxins, such as satratoxin G, roridin A, verrucarin A, and T-2 toxin (33, 34), and chitins in the outer wall of the spores. Chitins and β-glucans have been reported to induce a type 2 immune response (35). Lymphocytes, eosinophils, IL-13, and prostaglandins were much greater in the repeatedly exposed mice than in those exposed to mold only once, suggesting a switch from a type 1 immune response to a type 2 immune response. This switch might represent sensitization facilitated by repeated neutrophil influxes to the lungs in response to spores, as has been reported for ragweed (36). Prostaglandin D2, which is elevated in both single- and multiple-dosed mouse lungs, might be involved in recruitment of Th2 cells and eosinophils (37) seen in the multiple-dosed mice, but not the single-dosed mice.

Mice exposed to multiple doses of spores showed marked increases in many cytokines and metabolites compared with the mice that received only a single dose of *S. chartarum* spores. For some biomarkers, single-dosed mice were not significantly different from saline controls. The dose we used was 10- to 100-fold lower than those of our previous studies that used a single
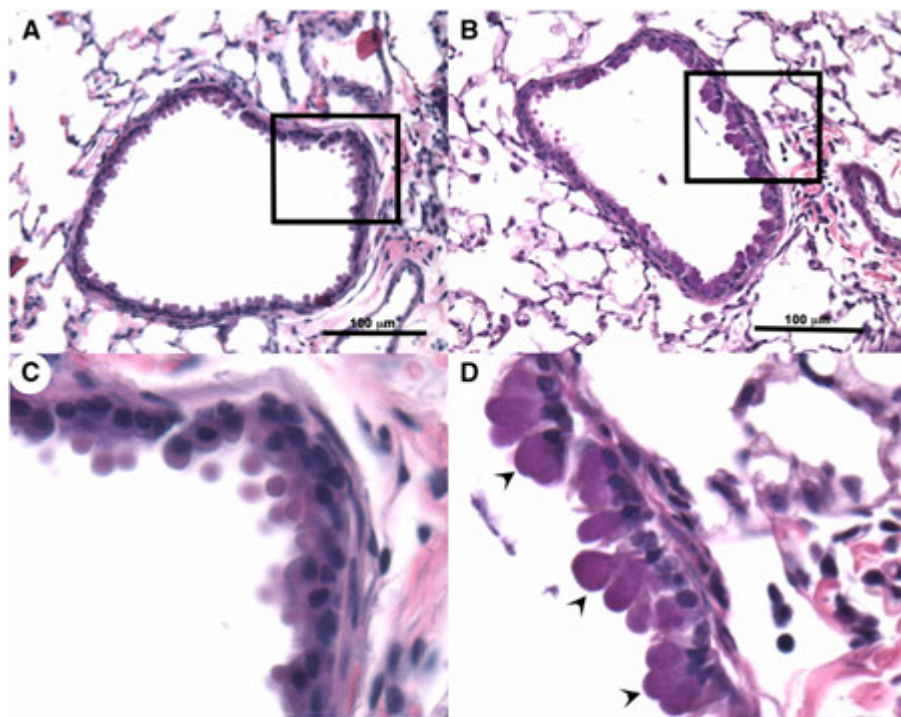
Figure 5. Histopathology of mouse lungs at 24 hours after final intratracheal instillation. (*A* and *C*) Periodic acid–Schiff (PAS)-stained section showing normal goblet cells in an airway from a single-dosed mouse lung. (*B* and *D*) PAS-stained section showing goblet cell metaplasia in an airway from a multiple-dosed mouse (*arrowheads*). (*C* and *D*) Higher magnification of enclosed areas in *A* and *B*. *Scale bar* = 100 μm.

instillation (13). Even when combined, the cumulative spore dose for the multiple-dosed group was still lower than the single dose of prior studies. We believe our results represent significant differences between single and multiple exposures (20, 38).

Pulmonary Cells

A similar degree of pulmonary inflammation was evident in both single- and multiple-dosed mice characterized by higher neutrophil influx. Interestingly, what distinguished the lung responses in the single- from multiple-dosed mice were the numbers of lymphocytes and eosinophils.

Eosinophils increased dramatically in the lungs, but decreased in the peripheral blood of multiple-dosed animals. This may represent the recruitment of eosinophils from the blood to the lungs after multiple exposures. Eotaxin, an eosinophil chemoattractant induced by IL-13 (39, 40), was highest in the lungs of multiple-dosed mice, and may have helped recruit eosinophils. The lymphocyte numbers in the BAL were also far greater in the multiple-dosed animals. In addition, we observed changes in lymphocyte populations recovered from dispersed lung tissues.

The type 2 (IL-13) and type 17 (IL-17) pathways likely mediate the eosinophil and neutrophil influx into the lungs seen in the multiple-dosed group, respectively. The type 2 and type 17 pathways have been shown to be important in the development of hypersensitivity pneumonitis from *S. chartarum* (41). The multiple-dosed group had increases in the numbers of CD45$^+$CD3$^-$IL-17A$^+$ cells compared with the single-dosed and unexposed controls. Although we did not stain the cells with the complete set of markers to define these cells as type 3 innate lymphoid cells (ILC) 3, based on the markers used and their forward and side scatter, we believe that the CD45$^+$CD3$^-$IL-17A$^+$ cells likely are ILC3 cells (32, 42–44). ILC3 cells have been shown to secrete IL-17 and IL-22 in the lungs in obesity (45), *Streptococcus pneumoniae* (46), and fungal infections (47, 48). These ILC3 cells may modulate the long-term inflammatory response to *S. chartarum*, and are likely key mediators of chronic inflammatory responses (49). Beause ILC2 has been shown to produce large amounts of type 2 cytokines, such as IL-5 and IL-15, and contribute to type 2 immunity (50–53), these cells could also be involved in the switch from type 1 to type 2 immune response in multiple-dosed mice. Airway epithelial cells might also be important mediators of pulmonary responses to *S. chartarum* (54). These potential mechanistic pathways should be incorporated into future studies.

Metabolic Changes

S. chartarum induced significantly more oxidative stress in the lungs of mice after multiple exposures than after a single exposure (Table E5). Glutathione metabolism was identified by pathway analysis (FDR q value = 5×10^{-5}) as the most impacted pathway in the lungs (Table 1). Glutathione metabolism plays a critical role in cytokine production, immune response, cell proliferation, and apoptosis (55). Increased levels of glutathione, in its reduced glutathione (GSH) and oxidized glutathione disulfide (GSSG) forms, may be associated with oxidative stress in lung tissue from mice exposed to *S. chartarum*. Higher glutathione levels might also be attributable to reduced degradation via the γ-glutamyl cycle rather than its increased synthesis.

S. chartarum induced an inflammatory signature that was more pronounced in the multiple-dosed compared with the single-dosed group. Arachidonic acid metabolism was identified as a key pathway stimulated by repeated *S. chartarum* doses (FDR q value = 5×10^{-5}). Arachidonic acid and its metabolites play a key role in regulating inflammatory responses (56). Included in the arachidonic acid pathway are prostaglandins that were enriched in the multiple-dosed mice versus single-dosed or control mice (Table E4). Prominent pathways identified among metabolites in the PCA also included those involving inflammatory prostaglandin-based and nucleotide synthesis pathways. Prostaglandins can enter the blood and mediate inflammatory responses in other organs (57). Significant changes emerged in metabolites in the plasma with SVM multimarker analysis, but not with pathway analysis or PCA. This suggests that SVM multimarker analysis is a more powerful way to distinguish multiple- and single-dosed mice when analyzing plasma data. All of the analytic methods showed clear
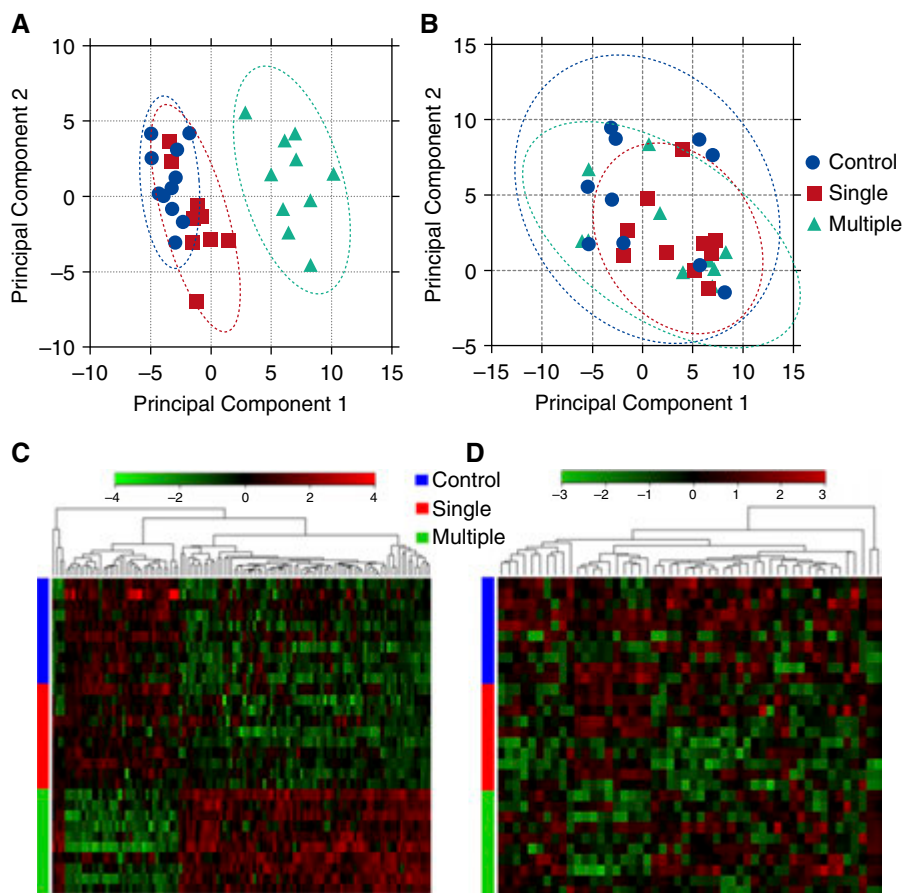
Figure 6. Principal component analysis of metabolites in the lung (*A*) and plasma (*B*). Ellipses represent 95% confidence interval. (*C*) Cluster analysis of 113 metabolites in the lungs with FDR *q* value < 0.05. (*D*) Cluster analysis of top 50 metabolites in plasma.

and consistent changes in the lungs of multiple-dosed mice.

Kynurenine, a tryptophan metabolite typically produced during inflammatory responses (58), was significantly elevated in multiple-dosed, but not in single-dosed, lungs. Tryptophan is primarily degraded in the liver by the enzyme tryptophan dioxygenase to kynurenine. The extrahepatic enzyme indoleamine 2,3-dioxygenase is highly inducible under inflammatory conditions and can also generate kynurenine from tryptophan. The significant elevation in kynurenine in lung tissues from mice subjected to multiple exposures to *S. chartarum* suggests increased inflammation in these animals.

Large increases in nucleotide metabolites (Table 1) may be associated with cell replication of eosinophils or lymphocytes, or cellular proliferation associated with airway remodeling, such as goblet cell hyperplasia. Significant reductions in essential and long-chain fatty

acids, along with lower levels of many ethanolamine- and choline-containing lysolipids, stearoyl sphingomyelin, and cholesterol, were observed in the lung tissue with repeated exposures to *S. chartarum*. The reductions in free fatty acids may be related to altered membrane remodeling/degradation rather than to changes in mitochondrial fatty acid oxidation. The potential exists that altered lung surfactant synthesis/secretion may contribute to these changes.

Altered Cytokines
Mice exposed to *S. chartarum* exhibited changes in IL-5, G-CSF, and KC in the plasma. These cytokines may also be altered in humans exposed to *S. chartarum* or other molds (9). IL-5 is associated with increased eosinophil response (59). High levels of IL-5 and eosinophils seen after multiple doses of *S. chartarum* may indicate an asthma-like response in these mice. IL-5 is also a marker of eosinophil activation. Its

presence in plasma was consistent with the high levels of eotaxin and eosinophils in the lungs. IL-5 has been shown to be required for persistence of eosinophils in the lungs (60). Eotaxin, predominately produced by epithelial and smooth muscle cells, is a well described chemoattractant for eosinophils (61). Furthermore, IL-13 is a major stimulant of eotaxin production (40).

Putative Metabolic Pathway-Cytokine Linkages
Several of the metabolic changes seen in this study after multiple exposures, but not with single exposures, to *S. chartarum* have been previously mechanistically linked with specific type 2 cytokine changes. It has been shown that key elements of a type 2 immune response, including IL-13–induced airway epithelial cell mucous cell hyperplasia, mucin and mucin-related gene expression, and airway hyperreactivity, are all glutathione dependent (62). The increase in activity in the glutamate metabolic pathway seen here is likely required for the shift from a type 1 to type 2 response. Glutamine metabolism, IL-4, and IL-13 work synergistically to increase rates of phagocytosis in a type 2 immune response (63). We see changes in metabolites, such as γ-glutamylglutamine that may be working with IL-13 and IL-4 to increase phagocytosis of *S. chartarum* spores.

Mouse–Human Data Correlations
Although species differences inevitably exist, a shift from a type 1 response to a type 2 response after chronic exposures can occur in both humans and animals. Our data also illustrate the importance of incorporating repeated exposures while studying pulmonary toxins, such as mold, in any species. Responses to acute exposures can be very different from those seen in more realistic repeated exposures. For example, acute exposure to ozone leads to a type 1 response, whereas repeated exposure leads to a type 2 response, but ozone exposures are often studied in naive mice and humans (64).

Our animal data also underscore the likely value of proteomic and metabolomic markers of exposures and responses in human studies. SVM analysis is a useful tool in selecting plasma biomarkers to identify individuals with a history of chronic mold exposures. Although the metabolites identified in our plasma SVM

Table 2. Support Vector Machine Analysis of Metabolites

Groups Separated	Metabolite	Super-Pathway	Sub-Pathway	Fold Change	P Value	AUC
Plasma: control versus single	2-Hydroxyisobutyrate	Xenobiotics	Chemical	0.89	0.001	0.893
	Adrenate	Lipid	Long-chain fatty acid	0.74	0.03	0.970
	Fructose	Carbohydrate	Fructose, mannose, galactose, starch, and sucrose metabolism	1.21	0.46	0.998
	Lactate	Carbohydrate	Glycolysis, gluconeogenesis, and pyruvate metabolism	0.92	0.49	0.999
	Adenosine 3′, 5′-cyclic monophosphate	Nuclotide	Purine metabolism	1.09	0.40	0.999
Plasma: control versus multiple	p-Cresol sulfate	Amino Acid	Phenylalanine and tyrosine metabolism	0.49	0.004	0.927
	Phenylacetylglycine	Amino Acid	Phenylalanine and tyrosine metabolism	0.63	0.09	0.942
	Glycerate	Carbohydrate	Glycolysis, gluconeogenesis, and pyruvate metabolism	1.10	0.29	0.965
	N-formylmethionine	Amino Acid	Cysteine, methionine, SAM, and taurine metabolism	0.78	0.66	0.965
	Stearoyl sphingomyelin	Lipid	Sphingolipid	0.84	0.05	0.980
Plasma: single versus multiple	Ectoine	Xenobiotics	Chemical	1.68	0.0002	0.920
	Tartarate	Xenobiotics	Food component/plant	1.63	0.004	1.000
Lung: control versus single	Ergothioneine	Xenobiotics	Food component/plant	1.65	9.2×10^{-7}	1.000
Lung: control versus multiple	7-β-Hydroxycholesterol	Lipid	Sterol/steroid	0.53	0.00004	1.000
Lung: single versus multiple	1-Stearoylglycero phosphoglycerol	Lipid	Lysolipid	1.65	0.0003	1.000

Definition of abbreviations: AUC, area under the curve; SAM, S-adenosyl-L-methionine.
AUCs listed are cumulative until the set includes 5 metabolites or a maximal AUC of 1.000 is reached. *P* values listed are for the individual metabolite.

analysis are biomarker candidates in humans, they must be validated in a larger study of plasma metabolites in subjects with documented chronic mold exposures and need to be compared with altered biomarkers seen for other pulmonary challenges.

We recently demonstrated several patterns of responses to mold in humans (9). Isolated human peripheral blood mononuclear cells were exposed to mycotoxins *ex vivo*. Subjects with a history of *S. chartarum* exposures showed altered levels of eotaxin, VEGF, MIP-1α, MIP-1β, and IL-8 compared with cells from control subjects. Here, we show that eotaxin,

VEGF, MIP-1α, MIP-1β, TNF-α, and the IL-8 analogs, MIP-2, KC (65), and LIX, were differentially expressed between singly and multiply exposed mice. Thus, many of the same biomarkers are implicated in both mice and humans.

Conclusions

Multiple doses of *S. chartarum* induced inflammatory responses and metabolomic profiles distinct from those induced by a single exposure and consistent with sensitization and changes in the immune response. These cellular, inflammatory, and metabolomic differences indicate that future studies should

focus on the consequences of multiple rather than single acute exposures. Caution should be exercised when interpreting responses to acute exposures in animal and human studies. ■

References

1. Brasel TL, Martin JM, Carriker CG, Wilson SC, Straus DC. Detection of airborne *Stachybotrys chartarum* macrocyclic trichothecene mycotoxins in the indoor environment. *Appl Environ Microbiol* 2005; 71:7376–7388.
2. Al-Ahmad M, Manno M, Ng V, Ribeiro M, Liss GM, Tarlo SM. Symptoms after mould exposure including *Stachybotrys chartarum*, and comparison with darkroom disease. *Allergy* 2010;65:245–255.
3. Ward MD, Copeland LB, Lehmann J, Doerfler DL, Vesper SJ. Assessing the allergenic potential of molds found in water-damaged homes in a mouse model. *Inhal Toxicol* 2014;26:474–484.
4. Baxi SN, Muilenberg ML, Rogers CA, Sheehan WJ, Gaffin J, Permaul P, Kopel LS, Lai PS, Lane JP, Bailey A, *et al*. Exposures to molds in school classrooms of children with asthma. *Pediatr Allergy Immunol* 2013;24:697–703.
5. Le U, Burks AW. Exposures to molds in school classrooms of children with asthma. *Pediatrics* 2014;134:S144.

6. Dearborn DG, Smith PG, Dahms BB, Allan TM, Sorenson WG, Montana E, Etzel RA. Clinical profile of 30 infants with acute pulmonary hemorrhage in Cleveland. *Pediatrics* 2002;110:627–637.

7. Shi C, Smith ML, Miller JD. Characterization of human antigenic proteins SchS21 and SchS34 from *Stachybotrys chartarum*. *Int Arch Allergy Immunol* 2011;155:74–85.

8. Straus DC. The possible role of fungal contamination in sick building syndrome. *Front Biosci (Elite Ed)* 2011;3:562–580.

9. Rosenblum Lichtenstein JH, Hsu YH, Gavin IM, Donaghey TC, Molina RM, Thompson KJ, Chi CL, Gillis BS, Brain JD. Environmental mold and mycotoxin exposures elicit specific cytokine and chemokine responses. *PLoS One* 2015;10: e0126926.

10. Hudson B, Flemming J, Sun G, Rand TG. Comparison of immunomodulator mRNA and protein expression in the lungs of *Stachybotrys chartarum* spore–exposed mice. *J Toxicol Environ Health A* 2005;68:1321–1335.

11. Rand TG, Miller JD. Immunohistochemical and immunocytochemical detection of SchS34 antigen in *Stachybotrys chartarum* spores and spore impacted mouse lungs. *Mycopathologia* 2008;165: 73–80.

12. Yike I, Rand TG, Dearborn DG. Acute inflammatory responses to *Stachybotrys chartarum* in the lungs of infant rats: time course and possible mechanisms. *Toxicol Sci* 2005;84:408–417.

13. Rosenblum Lichtenstein JH, Molina RM, Donaghey TC, Brain JD. Strain differences influence murine pulmonary responses to *Stachybotrys chartarum*. *Am J Respir Cell Mol Biol* 2006;35:415–423.

14. Lichtenstein JH, Molina RM, Donaghey TC, Amuzie CJ, Pestka JJ, Coull BA, Brain JD. Pulmonary responses to *Stachybotrys chartarum* and its toxins: mouse strain affects clearance and macrophage cytotoxicity. *Toxicol Sci* 2010;116:113–121.

15. Yike I, Rand T, Dearborn DG. The role of fungal proteinases in pathophysiology of *Stachybotrys chartarum*. *Mycopathologia* 2007; 164:171–181.

16. Viana ME, Coates NH, Gavett SH, Selgrade MK, Vesper SJ, Ward MD. An extract of *Stachybotrys chartarum* causes allergic asthma-like responses in a BALB/c mouse model. *Toxicol Sci* 2002;70:98–109.

17. Nagayoshi M, Tada Y, West J, Ochiai E, Watanabe A, Toyotome T, Tanabe N, Takiguchi Y, Shigeta A, Yasuda T, *et al*. Inhalation of *Stachybotrys chartarum* evokes pulmonary arterial remodeling in mice, attenuated by Rho-kinase inhibitor. *Mycopathologia* 2011;172: 5–15.

18. Leino MS, Alenius HT, Fyhrquist-Vanni N, Wolff HJ, Reijula KE, Hintikka EL, Salkinoja-Salonen MS, Haahtela T, Mäkelä MJ. Intranasal exposure to *Stachybotrys chartarum* enhances airway inflammation in allergic mice. *Am J Respir Crit Care Med* 2006; 173:512–518.

19. Ochiai E, Kamei K, Watanabe A, Nagayoshi M, Tada Y, Nagaoka T, Sato K, Sato A, Shibuya K. Inhalation of *Stachybotrys chartarum* causes pulmonary arterial hypertension in mice. *Int J Exp Pathol* 2008;89:201–208.

20. Brain JD, Knudson DE, Sorokin SP, Davis MA. Pulmonary distribution of particles given by intratracheal instillation or by aerosol inhalation. *Environ Res* 1976;11:13–33.

21. Skaper SD, Evans NA, Evans NA, Rosin C, Facci L, Richardson JC. Oligodendrocytes are a novel source of amyloid peptide generation. *Neurochem Res* 2009;34:2243–2250.

22. Ohta T, Masutomi N, Tsutsui N, Sakairi T, Mitchell M, Milburn MV, Ryals JA, Beebe KD, Guo L. Untargeted metabolomic profiling as an evaluative tool of fenofibrate-induced toxicology in Fischer 344 male rats. *Toxicol Pathol* 2009;37:521–535.

23. Suhre K, Meisinger C, Döring A, Altmaier E, Belcredi P, Gieger C, Chang D, Milburn MV, Gall WE, Weinberger KM, *et al*. Metabolic footprint of diabetes: a multiplatform metabolomics study in an epidemiological setting. *PLoS One* 2010;5:e13953.

24. Kasahara DI, Kim HY, Mathews JA, Verbout NG, Williams AS, Wurmbrand AP, Ninin FMC, Neto FL, Benedito LAP, Hug C, *et al*. Pivotal role of IL-6 in the hyperinflammatory responses to subacute ozone in adiponectin-deficient mice. *Am J Physiol Lung Cell Mol Physiol* 2014;306:L508–L520.

25. Kasahara DI, Kim HY, Williams AS, Verbout NG, Tran J, Si H, Wurmbrand AP, Jastrab J, Hug C, Umetsu DT, *et al*. Pulmonary inflammation induced by subacute ozone is augmented in adiponectin-deficient mice: role of IL-17A. *J Immunol* 2012;188: 4558–4567.

26. Laan M, Cui ZH, Hoshino H, Lötvall J, Sjöstrand M, Gruenert DC, Skoogh BE, Lindén A. Neutrophil recruitment by human IL-17 via C-X-C chemokine release in the airways. *J Immunol* 1999;162:2347–2352.

27. Sher A, Coffman RL, Hieny S, Scott P, Cheever AW. Interleukin 5 is required for the blood and tissue eosinophilia but not granuloma formation induced by infection with *Schistosoma mansoni*. *Proc Natl Acad Sci USA* 1990;87:61–65.

28. Kurup VP, Seymour BW, Choi H, Coffman RL. Particulate *Aspergillus fumigatus* antigens elicit a TH2 response in BALB/c mice. *J Allergy Clin Immunol* 1994;93:1013–1020.

29. Inagaki-Ohara K, Sakamoto Y, Dohi T, Smith AL. γδ T cells play a protective role during infection with *Nippostrongylus brasiliensis* by promoting goblet cell function in the small intestine. *Immunology* 2011;134:448–458.

30. Mathews JA, Williams AS, Brand JD, Wurmbrand AP, Chen L, Ninin FM, Si H, Kasahara DI, Shore SA. γδ T cells are required for pulmonary IL-17A expression after ozone exposure in mice: role of TNFα. *PLoS One* 2014;9:e97707.

31. Medema MH, Blin K, Cimermancic P, de Jager V, Zakrzewski P, Fischbach MA, Weber T, Takano E, Breitling R. antiSMASH: rapid identification, annotation and analysis of secondary metabolite biosynthesis gene clusters in bacterial and fungal genome sequences. *Nucleic Acids Res* 2011;39:W339-46.

32. Klein Wolterink RG, Hendriks RW. Type 2 innate lymphocytes in allergic airway inflammation. *Curr Allergy Asthma Rep* 2013;13:271–280.

33. Kankkunen P, Rintahaka J, Aalto A, Leino M, Majuri ML, Alenius H, Wolff H, Matikainen S. Trichothecene mycotoxins activate inflammatory response in human macrophages. *J Immunol* 2009;182:6418–6425.

34. de Carvalho MP, Weich H, Abraham W-R. Macrocyclic trichothecenes as antifungal and anticancer compounds. *Curr Med Chem* 2016;23:23–35.

35. Amarsaikhan N, Templeton SP. Co-recognition of β-glucan and chitin and programming of adaptive immunity to *Aspergillus fumigatus*. *Front Microbiol* 2015;6:344.

36. Hosoki K, Aguilera-Aguirre L, Brasier AR, Kurosky A, Boldogh I, Sur S. Facilitation of allergic sensitization and allergic airway inflammation by pollen-induced innate neutrophil recruitment. *Am J Respir Cell Mol Biol* 2015;54:81–90.

37. Hirai H, Tanaka K, Yoshie O, Ogawa K, Kenmotsu K, Takamori Y, Ichimasa M, Sugamura K, Nakamura M, Takano S, *et al*. Prostaglandin D2 selectively induces chemotaxis in T helper type 2 cells, eosinophils, and basophils via seven-transmembrane receptor CRTH2. *J Exp Med* 2001;193:255–261.

38. Beck BD, Brain JD, Bohannon DE. An *in vivo* hamster bioassay to assess the toxicity of particulates for the lungs. *Toxicol Appl Pharmacol* 1982;66:9–29.

39. Jose PJ, Griffiths-Johnson DA, Collins PD, Walsh DT, Moqbel R, Totty NF, Truong O, Hsuan JJ, Williams TJ. Eotaxin: a potent eosinophil chemoattractant cytokine detected in a guinea pig model of allergic airways inflammation. *J Exp Med* 1994;179:881–887.

40. Zhu Z, Homer RJ, Wang Z, Chen Q, Geba GP, Wang J, Zhang Y, Elias JA. Pulmonary expression of interleukin-13 causes inflammation, mucus hypersecretion, subepithelial fibrosis, physiologic abnormalities, and eotaxin production. *J Clin Invest* 1999;103:779–788.

41. Bhan U, Newstead MJ, Zeng X, Podsaid A, Goswami M, Ballinger MN, Kunkel SL, Standiford TJ. TLR9-dependent IL-23/IL-17 is required for the generation of *Stachybotrys chartarum*–induced hypersensitivity pneumonitis. *J Immunol* 2013;190:349–356.

42. Serafini N, Klein Wolterink RG, Satoh-Takayama N, Xu W, Vosshenrich CA, Hendriks RW, Di Santo JP. Gata3 drives development of RORγt⁺ group 3 innate lymphoid cells. *J Exp Med* 2014;211: 199–208.

43. Romera-Hernandez M, Aparicio-Domingo P, Cupedo T. Damage control: Rorγt⁺ innate lymphoid cells in tissue regeneration. *Curr Opin Immunol* 2013;25:156–160.

44. Killig M, Glatzer T, Romagnani C. Recognition strategies of group 3 innate lymphoid cells. *Front Immunol* 2014;5:142.

45. Kim HY, Lee HJ, Chang YJ, Pichavant M, Shore SA, Fitzgerald KA, Iwakura Y, Israel E, Bolger K, Faul J, *et al*. Interleukin-17–producing innate lymphoid cells and the NLRP3 inflammasome facilitate obesity-associated airway hyperreactivity. *Nat Med* 2014;20:54–61.

46. Van Maele L, Carnoy C, Cayet D, Ivanov S, Porte R, Deruy E, Chabalgoity JA, Renauld JC, Eberl G, Benecke AG, *et al*. Activation of Type 3 innate lymphoid cells and interleukin 22 secretion in the lungs during *Streptococcus pneumoniae* infection. *J Infect Dis* 2014; 210:493–503.

47. McKenzie AN, Spits H, Eberl G. Innate lymphoid cells in inflammation and immunity. *Immunity* 2014;41:366–374.

48. Becker KL, Ifrim DC, Quintin J, Netea MG, van de Veerdonk FL. Antifungal innate immunity: recognition and inflammatory networks. *Semin Immunopathol* 2015;37:107–116.

49. Eberl G, Colonna M, Di Santo JP, McKenzie AN. Innate lymphoid cells: a new paradigm in immunology. *Science* 2015;348:aaa6566.

50. Piehler D, Eschke M, Schulze B, Protschka M, Müller U, Grahnert A, Richter T, Heyen L, Köhler G, Brombacher F, *et al*. The IL-33 receptor (ST2) regulates early IL-13 production in fungus-induced allergic airway inflammation. *Mucosal Immunol* 2016;9:937–949.

51. Oczypok EA, Milutinovic PS, Alcorn JF, Khare A, Crum LT, Manni ML, Epperly MW, Pawluk AM, Ray A, Oury TD. Pulmonary receptor for advanced glycation end-products promotes asthma pathogenesis through IL-33 and accumulation of group 2 innate lymphoid cells. *J Allergy Clin Immunol* 2015;136:747–756.e4.

52. Huang Y, Guo L, Qiu J, Chen X, Hu-Li J, Siebenlist U, Williamson PR, Urban JF Jr, Paul WE. IL-25–responsive, lineage-negative KLRG1(hi) cells are multipotential 'inflammatory' type 2 innate lymphoid cells. *Nat Immunol* 2015;16:161–169.

53. Castanhinha S, Sherburn R, Walker S, Gupta A, Bossley CJ, Buckley J, Ullmann N, Grychtol R, Campbell G, Maglione M, *et al*. Pediatric severe asthma with fungal sensitization is mediated by steroid-resistant IL-33. *J Allergy Clin Immunol* 2015;136:312–22.e7.

54. Holtzman MJ. Arachidonic acid metabolism in airway epithelial cells. *Annu Rev Physiol* 1992;54:303–329.

55. Wu G, Fang YZ, Yang S, Lupton JR, Turner ND. Glutathione metabolism and its implications for health. *J Nutr* 2004;134:489–492.

56. Samuelsson B. Arachidonic acid metabolism: role in inflammation. *Z Rheumatol* 1991;50:3–6.

57. McGiff JC, Terragno NA, Strand JC, Lee JB, Lonigro AJ, Ng KKF. Selective passage of prostaglandins across the lung. *Nature* 1969;223:742–745.

58. Opitz CA, Litzenburger UM, Sahm F, Ott M, Tritschler I, Trump S, Schumacher T, Jestaedt L, Schrenk D, Weller M, *et al*. An endogenous tumour-promoting ligand of the human aryl hydrocarbon receptor. *Nature* 2011;478:197–203.

59. Cieslewicz G, Tomkinson A, Adler A, Duez C, Schwarze J, Takeda K, Larson KA, Lee JJ, Irvin CG, Gelfand EW. The late, but not early, asthmatic response is dependent on IL-5 and correlates with eosinophil infiltration. *J Clin Invest* 1999;104:301–308.

60. Yamaguchi Y, Hayashi Y, Sugama Y, Miura Y, Kasahara T, Kitamura S, Torisu M, Mita S, Tominaga A, Takatsu K. Highly purified murine interleukin 5 (IL-5) stimulates eosinophil function and prolongs *in vitro* survival: IL-5 as an eosinophil chemotactic factor. *J Exp Med* 1988;167:1737–1742.

61. Griffiths-Johnson DA, Collins PD, Rossi AG, Jose PJ, Williams TJ. The chemokine, eotaxin, activates guinea-pig eosinophils *in vitro* and causes their accumulation into the lung *in vivo*. *Biochem Biophys Res Commun* 1993;197:1167–1172.

62. Lowry MH, McAllister BP, Jean JC, Brown LA, Hughey RP, Cruikshank WW, Amar S, Lucey EC, Braun K, Johnson P, *et al*. Lung lining fluid glutathione attenuates IL-13–induced asthma. *Am J Respir Cell Mol Biol* 2008;38:509–516.

63. Biswas SK, Mantovani A. Orchestration of metabolism by macrophages. *Cell Metab* 2012;15:432–437.

64. Ong CB, Kumagai K, Brooks PT, Brandenberger C, Lewandowski RP, Jackson-Humbles DN, Nault R, Zacharewski TR, Wagner JG, Harkema JR. Ozone-induced type 2 immunity in nasal airways: development and lymphoid cell dependence in mice. *Am J Respir Cell Mol Biol* 2016;54:331–340.

65. Call DR, Nemzek JA, Ebong SJ, Bolgos GR, Newcomb DE, Wollenberg GK, Remick DG. Differential local and systemic regulation of the murine chemokines KC and MIP2. *Shock* 2001;15: 278–284.